The distorted wave Born approximation: application to elastodynamics

K. E. Newman, S. Teitel,[a] and E. Domany[b]
Department of Physics, University of Washington, Seattle, Washington 98195

(Received 11 October 1979; accepted for publication 4 September 1980)

An approximate theory for scattering of elastic waves by general shaped defects has been developed. A defect of arbitrary shape can be represented by a sphere S and a remainder volume $\bar{R}$. Using the exact solution for a sphere and treating $\bar{R}$ as a perturbation, the solution corresponding to the distorted wave Born approximation is obtained. This solution contains nontrivial frequency dependence and phase information. Preliminary comparisons with experiments are presented.

PACS numbers: 03.40.Dz, 62.20.Dc

I. INTRODUCTION

The problem of elastic wave scattering by material imperfections has received considerable attention in recent years. In particular, the possible use of ultrasonic waves to characterize defects has attracted theoretical and experimental attention.[1] The aim of these research efforts is to develop reliable inversion procedures[2,3] that yield properties of the defect such as location, composition, shape, and orientation.[4] The information thus obtained, together with fracture mechanics considerations,[5] can be used in the context of Nondestructive evaluation (NDE), to predict the lifetime of various parts, and to yield reliable accept-reject criteria.

To develop good inversion procedures, reliable solutions of the direct problem, namely, the ultrasonic power scattered by known defects, are most important. However, owing to the complexity of the problem, exact solutions are available only for a limited number of scatterer geometries.[6] Therefore theoretical analysis must rely on various approximation schemes.

A large number of approximation methods exists. The so-called quasistatic approximations[7] are valid for low frequencies only, i.e., when the wavelength $\bar{\lambda}$ of the incident elastic wave is much larger than the characteristic defect size a (i.e., $ka \ll 1$, where $k = 2\pi/\bar{\lambda}$). These approximations can be extended to yield reasonably reliable information up to $ka \approx 1$. However, in order to implement them, the solution of the static problem must be known; therefore these methods are limited to dealing with simple shapes only.

In the opposite limit, i.e., $ka \gg 1$, solutions based on expansion in $(ka)^{-1/2}$ were developed for scattering by cracks.[8] These solutions are based on ray tracing, and come under the name of "geometrical theory of diffraction." Analytic expressions obtained by this method indicate that the regime of validity may extend to the intermediate ka regime. However, so far for elastic waves the approach is limited to cracks only.

The first Born approximation[9] was used extensively to extract information about the physical features of the scattered power that are relevant for defect characterization. This approximation, however, is valid only in the limit of very weak scattering; for strong scatterers (such as cavities) the region of validity is for $ka \lesssim 1$, the frequency dependence of the scattered power is unreliable, and so is the phase information.

A rather promising approach is that of truncated eigenfunction expansions.[10,11] Although methods based on this approach yield reliable information for a wide range of ka, available computer storage space limits their use to defects that possess axial symmetry.

We have set out to formulate an approximation to the elastic wave scattering problem that yields reliable frequency dependence and phase information in the low and intermediate ka regimes for quite general shaped volume defects. We hope that such an approximation will be useful to study effects of nonregular defect surfaces and yield data to be used in inversion procedures. We also hope to use the results to check concepts such as an "effective spheroid" that has been suggested to represent general shaped defects.

Our approximation scheme differs from the existing ones in that it uses *shape perturbations* as a small parameter—namely, the deviation of the actual defect shape from spherical. We use the exactly soluble case[12] of scattering by a sphere as our zeroth-order approximate solution. To calculate the approximate solution to first order in the shape perturbation, we use these exact solutions. This procedure is an adaptation of the distorted wave Born approximation[13] (DWBA) to elastodynamics.

The general formalism is presented in Sec. II. As shown there, one needs the Green's function of an infinite medium with a spherical defect. This Green's function is needed only in the asymptotic far field regime; its evaluation in terms of plane waves scattered by a sphere is given in Sec. III. The

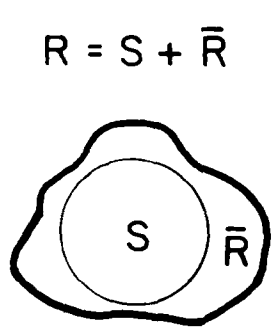

FIG. 1. A general shaped defect R can be represented as a spherical defect S and a "remainder" volume $\bar{R}$.

[a]Permanent address: Department of Physics, Cornell University, Ithaca, New York.

[b]Permanent address: Department of Electronics, Weizmann Institute of Science, Rehovot, Israel.

 0021-8979/81/074363-08$01.10

Green's function is incorporated in the DWBA expression and the far field scattering amplitudes are presented in Sec. IV, where numerical checks and results for a nonspherical defect are also given. Section V summarizes our results, with special emphasis on possible uses in the NDE context.

II. THE DISTORTED WAVE BORN APPROXIMATION: GENERAL FORMALISM

The DWBA is based on a perturbative solution of the integral equation for the scattered field. A derivation of the volume integral formulation of the elastodynamic scattering problem was presented by Gubernatis *et al.*[14] In this paper we follow the notation of that reference.

Consider the differential equation for the propagation of elastic waves in a medium, characterized by (position dependent) elastic tensor C_{ijkl} and density, ρ, given by

$$(C_{ijkl}u_{k,l})_{,j} + \rho\omega^2 u_i = 0, \tag{2.1}$$

where u_i is the displacement field and $\omega/2\pi$ the frequency. Repeated indices are summed over; the symbol $a_{,j}$ stands for $\partial a/\partial x_j$. When spherical coordinates are used, we will employ notation such as $a_{,r}$ for $\partial a/\partial r$. We assume that a single defect is embedded in an infinite medium; both defect and medium are isotropic, e.g.,

$$C_{ijkl} = \lambda\delta_{ij}\delta_{kl} + \mu(\delta_{ik}\delta_{jl} + \delta_{il}\delta_{jk}).$$

The geometry of the problem is shown in Fig. 1. The coordinate dependence of C_{ijkl} and ρ can be expressed as

$$\begin{aligned} C(\mathbf{r}) &= C^0 + \theta_R(\mathbf{r})\delta C, \\ \rho(r) &= \rho^0 + \theta_R(\mathbf{r})\delta\rho, \end{aligned} \tag{2.2}$$

where $\theta_R(\mathbf{r}) = 1$, if $\mathbf{r}\in R$, and zero otherwise. The defect R is separated into two regions: a spherical one (S) and a remainder volume $\bar{R}$,[15] such that $R = S + \bar{R}$. The one can define functions $\theta_S(\mathbf{r})$ and $\theta_{\bar{R}}(\mathbf{r})$, so that

$$\theta_R(\mathbf{r}) = \theta_S(\mathbf{r}) + \theta_{\bar{R}}(\mathbf{r}). \tag{2.3}$$

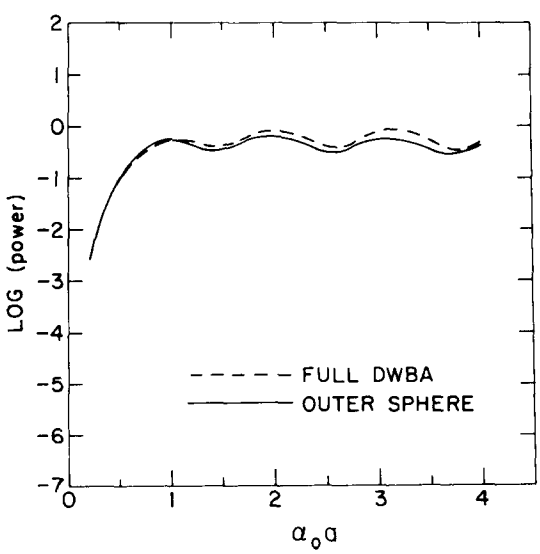

FIG. 2. Backscattered longitudinal power from a spherical cavity of radius a, in Ti, for incident longitudinal waves of wave number α_0. Exact results (solid line) are compared with the results of the DWBA, obtained from the solution of a smaller sphere of radius $5a/6$, and treating the difference between the two spheres as a perturbation.

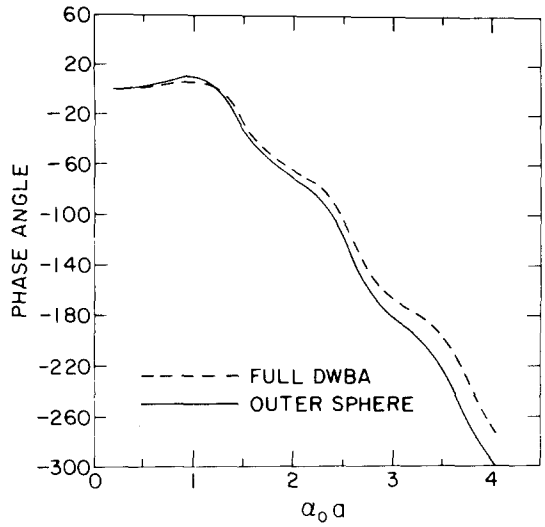

FIG. 3. Phase angle of the backscattered longitudinal wave from a spherical cavity of radius a, in Ti, for incident longitudinal waves of wave number α_0. Exact results (solid line) are compared with the results of the DWBA, obtained from the solution of a smaller sphere of radius $5a/6$, and treating the difference between the two spheres as a perturbation.

We now consider as our unperturbed problem the case where only the spherical defect S is present. To do this, define

$$\begin{aligned} C^S(\mathbf{r}) &= C^0 + \theta_S(\mathbf{r})\delta C, \\ \rho^S(\mathbf{r}) &= \rho^0 + \theta_S(\mathbf{r})\delta\rho, \end{aligned} \tag{2.4}$$

and we can obviously write

$$\begin{aligned} C(\mathbf{r}) &= C^S(\mathbf{r}) + \theta_{\bar{R}}(\mathbf{r})\delta\, C, \\ \rho(\mathbf{r}) &= \rho^S(\mathbf{r}) + \theta_{\bar{R}}(\mathbf{r})\delta\rho. \end{aligned} \tag{2.5}$$

Using now (2.5) in (2.1), the scattering equation takes the form

$$\begin{aligned} (C^S_{ijkl}u_{k,l})_{,j} + \rho^S\omega^2 u_i = &-\theta_{\bar{R}}\delta\omega^2 u_i \\ &- (\theta_{\bar{R}}\delta C_{ijkl}u_{k,l})_{,j}. \end{aligned} \tag{2.6}$$

If the right-hand side of (2.6) is zero, the solutions of this equation are the waves scattered by a spherical defect, obtained previously by various authors. These solutions are readily evaluated numerically. To introduce notation used later, the solution of the spherical scattering problem, evaluated at point $\mathbf{r}$, corresponding to an incident wave with wave vector $\mathbf{k}$ and polarization ϵ is denoted by $u_i^S(\mathbf{r},\mathbf{k},\epsilon)$.

The solution of Eq. (2.1) or (2.2) satisfies an integral equation. The derivation of such a volume integral equation was discussed in detail by Gubernatis, Domany, and Krumhansl,[14] to which the interested reader is referred. Here we only mention that standard boundary conditions are used, i.e., continuity of displacement and normal stress (for elastic inclusions) and vanishing normal stress (on the surface of a cavity), together with $\mathbf{u}(\mathbf{r})\to\mathbf{u}^0(\mathbf{r})$ as $r\to\infty$, where $\mathbf{u}^0$ is the incident field.

Proceeding in a similar fashion as Gubernatis *et al.*,[14] we obtain the following integral equation for the solution of (2.1) or (2.6):

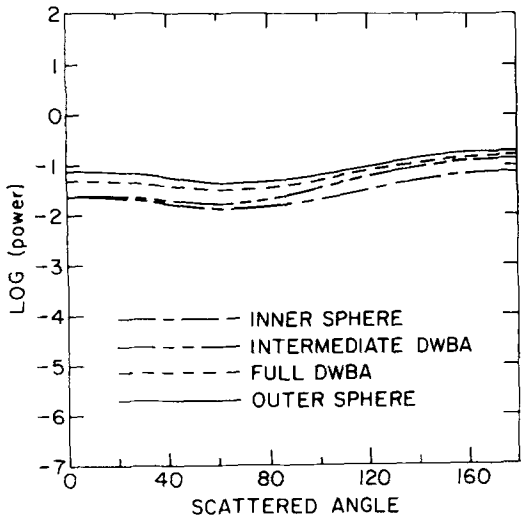

FIG. 4. Longitudinal power vs scattering angle for a spherical cavity of radius a in Ti, and incident longitudinal wave of wave number $\alpha_0 = 0.6/a$. The exact result (solid line) is compared with that obtained for a spherical cavity of radius $5a/6$; the difference between "full" and "intermediate" DWBA is discussed in the paragraph that follows Eq. (4.9).

$$u_i(\mathbf{r},\mathbf{k},\epsilon) = u_i^S(\mathbf{r},\mathbf{k},\epsilon) + \delta\rho\omega^2 \int_{\bar{R}} d\mathbf{r}' g_{im}^S(\mathbf{r},\mathbf{r}') u_m(\mathbf{r}',\mathbf{k},\epsilon) - \delta C_{jklm} \int_{\bar{R}} d\mathbf{r}' g_{ij,k'}^S(\mathbf{r},\mathbf{r}') u_{l,m'}(\mathbf{r}',\mathbf{k},\epsilon), \quad (2.7)$$

where $u_{l,m'} = \partial u_l / \partial x'_m$.

Note that the integration extends over the remainder region $\bar{R}$ only, and that the Green's function that appears in the integrand is $g_{ij}^S(\mathbf{r},\mathbf{r}')$, the spherical Green's function. This function is the solution of the equation

$$C_{ijkl} g_{km,jl}^S + \rho^S \omega^2 g_{im}^S = -\delta_{im}\delta(\mathbf{r}-\mathbf{r}'). \quad (2.8)$$

The spherical Green's function describes the response at point $\mathbf{r}$ to a point-source force field located at point $\mathbf{r}'$, in an infinite medium in which a spherical defect is embedded. Note that since C^S and ρ^S are not translationally invariant, $g^S(\mathbf{r},\mathbf{r}')$ is *not* function of the difference $\mathbf{r}-\mathbf{r}'$ only. Only a single component of this function has been derived previously.[16] The *exact* integral equation (2.7) serves as the starting point of our approximation procedure. The scattered field $u_i(\mathbf{r},\mathbf{k},\epsilon)$ can be expanded in a power series in the volume perturbation $\bar{R}$; to *first order*, the solution is given by

$$u_i^{\mathrm{DWBA}}(\mathbf{r},\mathbf{k},\epsilon) = u_i^S(\mathbf{r},\mathbf{k},\epsilon) + \delta\rho\omega^2 \int_{\bar{R}} g_{im}^S(\mathbf{r},\mathbf{r}') u_m^S(\mathbf{r}',\mathbf{k},\epsilon) - \delta C_{jklm} \int_{\bar{R}} d\mathbf{r}' g_{ij,k'}^S(\mathbf{r},\mathbf{r}') u_{l,m'}^S(r',k,\epsilon). \quad (2.9)$$

This is the distorted wave Born approximation. It is analogous to the first Born approximation (BA). However, the BA uses the defect-free infinite medium as the zeroth-order approximation, and treats the *entire* defect as a perturbation. In contrast, the DWBA uses the scattering by a sphere S as the zeroth-order solution; only deviation from S, namely $\bar{R}$ is treated perturbatively.

The aim of our theory is to yield an expression for $u_i(\mathbf{r})$ in the far field, (i.e., $\mathbf{r}\to\infty$) limit. Many experimental situations correspond to this limit (i.e., when the source and receiver are at a distance r much larger than the wavelength $\bar{\lambda}$ or the defect size a). In this limit, the scattered displacement field has the form

$$u_i(\mathbf{r}) = \hat{r}_i A e^{i\alpha_0 r}/r + (\hat{\theta}_i B_\theta + \hat{\phi}_i B_\phi) e^{i\beta_0 r}/r, \quad (2.10)$$

where α_0 and β_0 are the longitudinal and shear wave numbers.

Since we are interested only in the far field limit, we need $g_{ij}^S(\mathbf{r},\mathbf{r}')$ only in the limit $\mathbf{r}\to\infty$ (i.e., response at ∞ to point source at $\mathbf{r}'$ near the sphere). In this limit we were able to evaluate $g_{ij}^S(\mathbf{r},\mathbf{r}')$, and therefore the amplitudes A, B_θ, and B_ϕ in the DWBA.

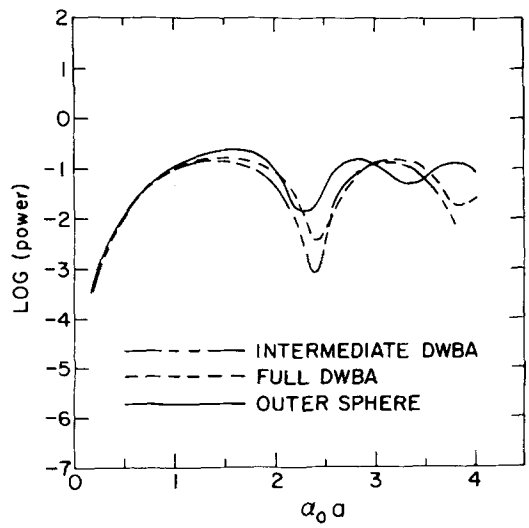

FIG. 5. Longitudinal backscattered power from an Al sphere of radius a in Ti, for incident longitudinal waves of wave number α_0. Exact results (solid line) are compared with those of the "full" and "intermediate" DWBA, obtained from the solution of a smaller sphere of radius $\frac{1}{2}a$, and treating the difference between the two spheres as a perturbation.

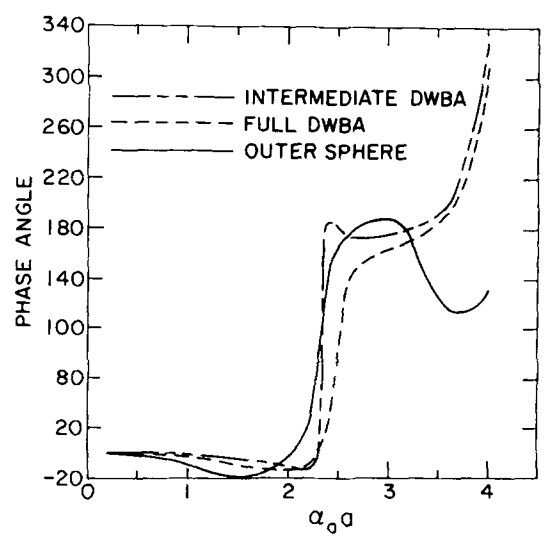

FIG. 6. Phase angle of backscattered longitudinal waves from an Al sphere of radius a in Ti, for incident longitudinal waves of wave number α_0. Exact results (solid line) are compared with those of the "full" and "intermediate" DWBA, obtained from the solutions of a smaller sphere of radius $\frac{1}{2}a$, and treating the difference between the two spheres as a perturbation.

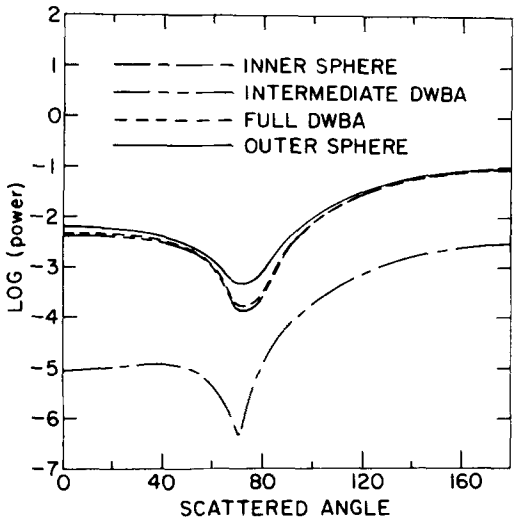

FIG. 7. Scattered longitudinal power, as a function of the scattering angle, for Al sphere of radius a in Ti, with $\alpha_0 = 1$. Exact results (solid line) are compared with the "full" and "intermediate" DWBA, based on an Al sphere of radius $\frac{1}{2}a$. The scattered power from this "inner sphere" is also shown.

III. THE SPHERICAL GREEN'S FUNCTION

To evaluate $g_{ij}(\mathbf{r},\mathbf{r}')$ we use the principles of superposition and reciprocity.[17] Our method yields the function for $\mathbf{r}\to\infty\hat{r}$, which is precisely the one needed in Eq. (2.10) since the point of observation, $\mathbf{r}$, is assumed to be at infinity for calculation of scattering amplitudes and cross sections.

First note that if the infinite medium Green's function $g^0(\mathbf{r}',\mathbf{r})$ can be expanded in terms of plane waves,

$$g^0_{ij}(\mathbf{r}',\mathbf{r}) = \sum_{\epsilon}\int d\,\mathbf{k} A_j(\mathbf{r},\mathbf{k},\epsilon) u^0_i(\mathbf{r}',\mathbf{k},\epsilon), \tag{3.1}$$

where $u^0_i(\mathbf{r}',\mathbf{k},\epsilon)$ are plane wave solutions of the (homogeneous medium) wave equation, the spherical Green's function will be given by

$$g^S_{ij}(\mathbf{r}',\mathbf{r}) = \sum_{\epsilon}\int d\,\mathbf{k} A_j(\mathbf{r},\mathbf{k},\epsilon) u^S_i(\mathbf{r}',\mathbf{k},\epsilon), \tag{3.2}$$

where $u^S_i(\mathbf{r}',\mathbf{k},\epsilon)$ is the solution of scattering the incident plane wave $u^0_i(\mathbf{r}',\mathbf{k},\epsilon)$ off a sphere. (The index ϵ stands for the various possible polarizations.) Therefore, once the expansion coefficient $A_j(\mathbf{r},\mathbf{k},\epsilon)$ are known, the spherical Green's function can be constructed, in principle, by superposition of solutions for the incident plane wave scattering problem. In general it is not trivial to find the $A_j(r,k,\epsilon)$ needed to expand $g^0_{ij}(\mathbf{r}',\mathbf{r})$; however, when the "source" position $\mathbf{r}\to\infty\hat{r}$, the expansion for the A_j is simple. To see this, note[14]

$$4\pi\rho_0\omega^2 g^0_{ij}(\mathbf{r}',\mathbf{r}) = \frac{\delta_{ij}\beta_0^2 e^{i\beta_0 R}}{R} - \partial_i\partial_j\left(\frac{e^{i\alpha_0 R}}{R} - \frac{e^{i\beta_0 R}}{R}\right), \tag{3.3}$$

with $R = |\mathbf{r}-\mathbf{r}'|$, $\partial_j = \partial/\partial x_j$, and $\alpha_0^2 = \rho_0\omega^2/(\lambda_0+2\mu_0)$, $\beta_0^2 = \rho_0\omega^2/\mu_0$. In the limit $\mathbf{r}\to\infty\hat{r}$, this expression becomes

$$4\pi\rho_0\omega^2 g^0_{ij}(\mathbf{r}',\mathbf{r}) = \beta_0^2\frac{e^{i\beta_0 r}}{r}e^{-\beta_0\hat{r}\cdot\mathbf{r}'}(\delta_{ij}-\hat{r}_i\hat{r}_j) + \alpha_0^2\frac{e^{i\alpha_0 r}}{r}e^{i\alpha_0\hat{r}\cdot\mathbf{r}'}\hat{r}_i\cdot\hat{r}_j\,. \tag{3.4}$$

Introducing now three unit vectors $\hat{e}^{\epsilon}$; $\hat{e}^1 = \hat{r}$, $\hat{e}^2 = \hat{\theta}$, and $\hat{e}^3 = \hat{\phi}$, this reads

$$4\pi\rho_0\omega^2 g^0_{ij}(\mathbf{r}',\mathbf{r}\to\infty\hat{r}) = \beta_0^2\,(e^{i\beta_0 r}/r)e^{-i\beta_0\hat{r}\cdot\hat{r}'}(\hat{e}^2_j\hat{e}^2_i + \hat{e}^3_j\hat{e}^3_i) + \alpha_0^2(e^{i\alpha_0 r}/r)e^{-i\alpha_0\hat{r}\cdot\mathbf{r}'}\hat{e}^1_j\hat{e}^1_i. \tag{3.5}$$

This expression has the form of (3.1), with only three incident plane waves

$$\mathbf{u}^0(\mathbf{r}',\mathbf{k},\epsilon) = \hat{e}^{\epsilon}e^{-i\gamma_0(\epsilon)\hat{r}\cdot\mathbf{r}'}, \tag{3.6}$$

needed to expand g^0. The coefficients A_j can be read off as given by

$$A_j(\mathbf{r},\mathbf{k},\epsilon) = \frac{1}{4\pi\rho_0\omega^2}\hat{e}^{\epsilon}_j\frac{e^{ikr}}{r}k^2\delta[\mathbf{k}+\gamma_0(\epsilon)\hat{r}], \tag{3.7}$$

where

$$\gamma_0(1) = \alpha_0, \quad \gamma_0(2) = \gamma_0(3) = \beta_0. \tag{3.8}$$

Finally, in this limit, the spherical Green's function reads

$$4\pi\rho_0\omega^2 g^S_{ij}(\mathbf{r}',\mathbf{r}\to\infty\hat{r}) = \sum_{\epsilon}\hat{e}^{\epsilon}_j\frac{e^{i\gamma_0(\epsilon)r}}{r}\gamma_0(\epsilon)^2 u^S_i[\mathbf{r}', -\gamma_0(\epsilon)\hat{r},\epsilon] \tag{3.9}$$

where $u^S_i[\mathbf{r}', -\gamma_0(\epsilon)r,\epsilon]$ is the solution for scattering by a sphere of a plane wave with polarization ϵ, wavevector $\gamma_0(\epsilon)$, incident in the $-\hat{r}$ direction, evaluated at point $\mathbf{r}'$.

Inspecting Eq. (2.9) we note that in order to evaluate $u^{\mathrm{DWBA}}(\mathbf{r})$ in the far field, i.e., $\mathbf{r}\to\infty$, we need g^S with the *point of observation* at ∞. To obtain this function, we use reciprocity,[17] e.g.,

$$g_{ij}(\mathbf{a},\mathbf{b}) = g_{ji}(\mathbf{b},\mathbf{a}), \tag{3.10}$$

to get

$$g^S_{ji}(\mathbf{r}\to\infty,\mathbf{r}') = \frac{1}{4\pi\rho_0\omega^2}\sum_{\epsilon}\hat{e}^{\epsilon}_j\frac{e^{i\gamma_0(\epsilon)r}}{r}\gamma_0(\epsilon)^2 \times u^S_i[\mathbf{r}', -\gamma_0(\epsilon)\hat{r},\epsilon]. \tag{3.11}$$

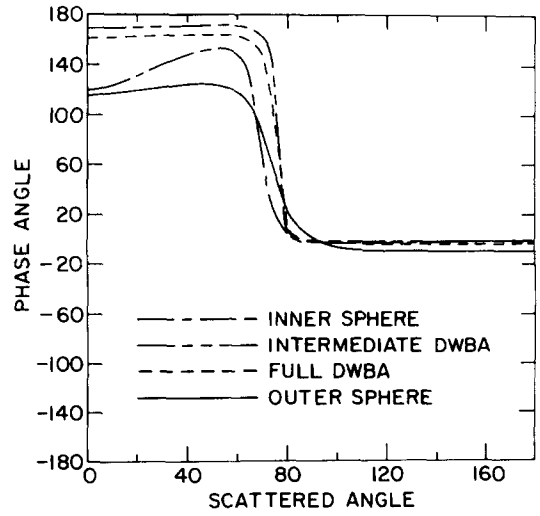

FIG. 8. Phase angle of scattered longitudinal wave as a function of the scattering angle, for Al sphere of radius a in Ti, with $\alpha_0 = 1$. Exact results (solid line) are compared with the "full" and "intermediate" DWBA, based on an Al sphere of radius $\frac{1}{2}a$.

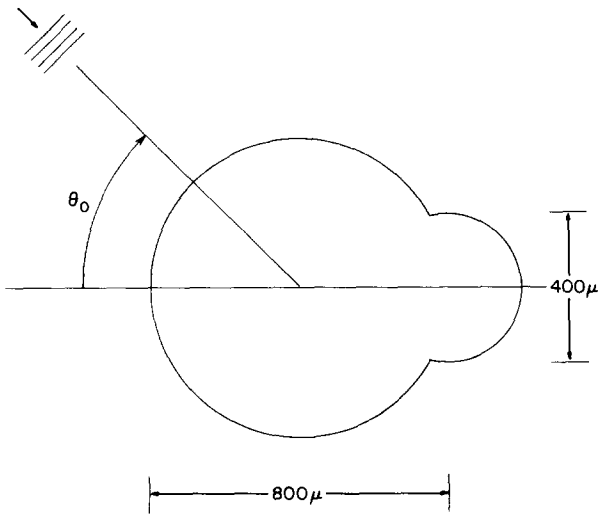

FIG. 9. Nonspherical defect; spherical cavity of radius 400 μ in Ti, to which a hemisphere of radius 200 μ has been added. Direction of incidence is denoted by θ_0.

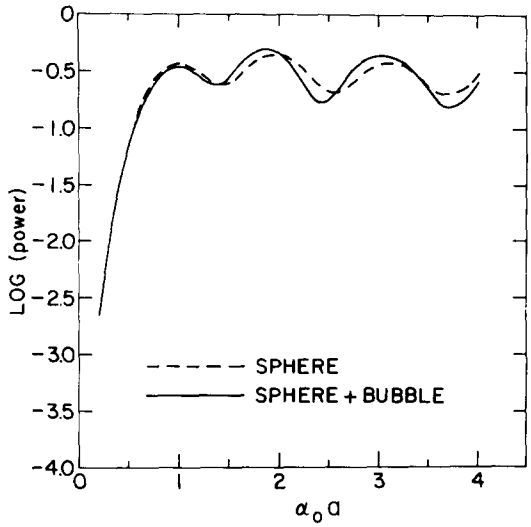

FIG. 10. Longitudinal backscattered power from the defect of Fig. 9, vs $\alpha_0 a$, where a is the radius of the large sphere and α_0 the wave number of the incident longitudinal wave. The angle of incidence is $\theta_0 = 0$, i.e., the "bubble" is shadowed by the sphere. Scattering from the sphere only is shown for comparison.

IV. THE DISTORTED WAVE BORN APPROXIMATION—FAR FIELD SCATTERING

Equation (3.11) is exactly the result needed to obtain displacement amplitudes for $\mathbf{r}\to\infty\hat{r}$. Inserting it into Eq. (2.9) one obtains for a plane wave incident along the $-\hat{r}^0$ direction, with polarization ϵ^0 and wave vector $-\gamma_0(\epsilon^0)\hat{r}_0$:

$$\vec{\mathbf{u}}^{\mathrm{DWBA}}[\mathbf{r}, -\gamma_0(\epsilon^0)\hat{r}^0,\epsilon^0] = \vec{\mathbf{u}}^S[\mathbf{r}, -\gamma_0(\epsilon^0)\hat{r}^0,\epsilon^0] + \sum_{\epsilon}\hat{e}^{\epsilon}\gamma_0(\epsilon)^2\frac{e^{i\gamma_0(\epsilon)r}}{r} \times(D_1+D_2+D_3), \tag{4.1}$$

where

$$D_1 = \frac{\delta\rho}{4\pi\rho_0}\int_{\bar{R}} d\mathbf{r}' u_m^S[\mathbf{r}', -\gamma_0(\epsilon)\hat{r},\epsilon], \times u_m^S(\mathbf{r}', -\gamma_0(\epsilon^0)\hat{r}^0,\epsilon^0),$$

$$D_2 = -\frac{\delta\lambda}{4\pi\rho_0\omega^2}\int_{\bar{R}} d\mathbf{r}' u^S_{m,m'}[r', -\gamma_0(\epsilon)\hat{r},\epsilon] \times u^S_{l,l'}[\mathbf{r}', -\gamma_0(\epsilon^0)\hat{r}^0,\epsilon^0]$$

$$D_3 = \frac{-2\delta\mu}{4\pi\rho_0\omega^2}\int_{\bar{R}} d\mathbf{r}' e^S_{jk}[\mathbf{r}', -\gamma_0(\epsilon)\hat{r},\epsilon] \times e^S_{jk}[\mathbf{r}', -\gamma_0(\epsilon^0)\hat{r}^0,\epsilon^0], \tag{4.2}$$

with

$$e^S_{jk} = 1/2[u^S_{j,k'} + u^S_{k,j'}].$$

The form of Eq. (4.1) is quite easy to interpret. The contribution of the volume perturbation $\bar{R}$ to the scattering appears in the proper far field form, with the well-defined independent polarizations $\hat{e}^{\epsilon} = (\hat{r},\hat{\theta},\hat{\phi})$. The amplitudes associated with these polarizations are expressed in terms of the spherical scattered solutions for two incident plane waves; one is the real physical incident wave, and the second a plane wave incident along the direction of observation, with the polarization of the desired scattered wave. The integrands are the appropriate scalars, that can be constructed from two such vector fields in a symmetric manner. The constants D depend on the incident and scattered directions and polarizations.

In this paper we concentrate only on the calculation of the longitudinal scattered amplitude A [as defined in Eq. (2.10)] from an incident longitudinal plane wave, $\hat{z}e^{i\alpha_0 z}$. The spherical scattering solution for elastic inclusions may be written in a notation similar to that of the Johnson-Truell solution[12]:

$$\mathbf{u}^S(\mathbf{r},\alpha_0\hat{z},\hat{z}) = \begin{cases}\hat{z}e^{i\alpha_0 z} - \nabla\psi^{\mathrm{out}} + \nabla x(\nabla x(\mathbf{r}\pi^{\mathrm{out}}))r > a\\ -\nabla\psi^{\mathrm{in}} + \nabla x(\nabla x(\mathbf{r}\pi^{\mathrm{in}}))\ r < a\end{cases} \tag{4.3}$$

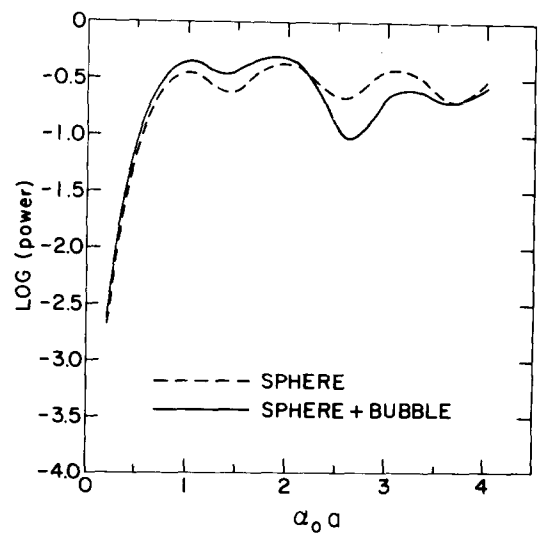

FIG. 11. Longitudinal backscattered power from the defect of Fig. 9, vs $\alpha_0 a$, where a is the radius of the large sphere and α_0 the wave number of the incident longitudinal wave. The angle of incidence is $\theta_0 = 90°$, i.e., side view of the "bubble."

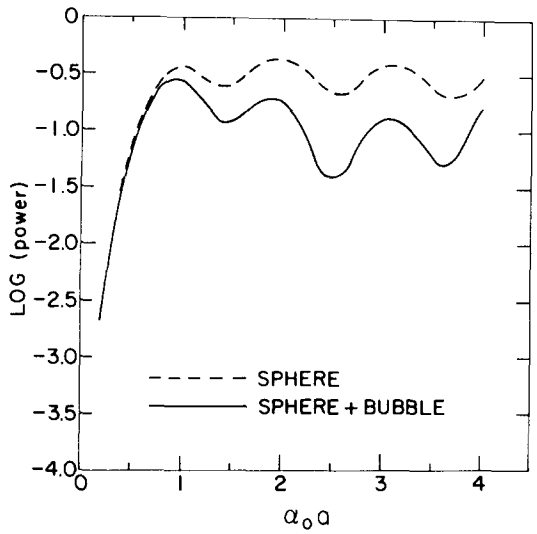

FIG. 12. Longitudinal backscattered power from the defect of Fig. 9, vs $\alpha_0 a$, where a is the radius of the large sphere and α_0 the wave number of the incident longitudinal wave. The angle of incidence is $\theta_0 = 0$, i.e., the "bubble" is illuminated directly.

where

$$\psi^{(\text{out})}_{(\text{in})} = \sum_{m=0} i^{m+1} a(2m+1) \begin{pmatrix} A_m \\ C_m \end{pmatrix} \begin{pmatrix} h_m^{(1)}(\alpha_0 r) \\ j_m(\alpha_1 r) \end{pmatrix} P_m(\cos\theta)$$

$$\pi^{(\text{out})}_{(\text{in})} = \sum_{m=0} i^{m+1} a(2m+1) \begin{pmatrix} B_m \\ D_m \end{pmatrix} \begin{pmatrix} h_m^{(1)}(\beta_0 r) \\ j_m(\beta_1 r) \end{pmatrix} P_m(\cos\theta) \tag{4.4}$$

Here a refers to the radius of the sphere, and the subscripts 0 and 1 refer to the regions outside and inside the sphere. Note that our plane wave is a complex conjugate of that used by Johnson and Truell.[12] Note also that as defined $\mathbf{u}^S$ is a dimensionless quantity; the incident amplitude has been factored out. In the same spirit, we define a scattering amplitude $\bar{A}$, which is a dimensionless form of A normalized by the plane wave and by the radius of the sphere. Then the longitudinal part of the scattered field, as given in Eq. (4.1), has the dimensionless amplitude

$$\bar{A} = \bar{A}^S + (\alpha_0^2/a)(D_1 + D_2 + D_3), \tag{4.5}$$

where[12]

$$\bar{A}^S = -i \sum_{m=0} (2m+1) A_m P_m(\cos\theta). \tag{4.6}$$

The longitudinal differential cross section in dimensionless units is given by[14]

$$\frac{dP_{\text{Long}}}{d\Omega} = |\bar{A}|^2, \tag{4.7}$$

and a phase angle δ can be defined by

$$\tan\delta = \text{Im}\bar{A}/\text{Re}\bar{A}. \tag{4.8}$$

The integrands D_1, D_2, and D_3 are found in terms of the derivatives of the functions ψ and π of Eq. (4.3). It is possible to check the correctness of the computer code for these integrals and for the spherical coefficients A_m to D_m by using Eq. (2.7). In this check $\bar{R}$ is taken to be a spherical shell from radius a_1 to radius a_2. Then, *exactly*, one may write

$$\bar{A}^{S_2} = \bar{A}^{S_1} + (\alpha_0^2/a_1)(D_1' + D_2' + D_3'), \tag{4.9}$$

where

$$D_1' = \frac{\delta\rho}{4\pi\rho_0} \int_{\text{shell}} d\mathbf{r}' u_m^{S_1}(\mathbf{r}', -\alpha_0\hat{r}^0, -\hat{r}^0) \times u_m^{S_2}(\mathbf{r}', \alpha_0\hat{z}, \hat{z})$$

$$D_2' = \frac{-\delta\lambda}{4\pi\rho_0\omega^2} \int_{\text{shell}} d\mathbf{r}' u_{l,l}^{S_1}(\mathbf{r}', -\alpha_0\hat{r}^0, -\hat{r}^0) \times u_{m,m'}^{S_2}(\mathbf{r}', \alpha_0\hat{z}, \hat{z})$$

$$D_3' = \frac{-2\delta\mu}{4\pi\rho_0\omega^2} \int_{\text{shell}} d\mathbf{r}' e_{jk}^{S_1}(\mathbf{r}', -\alpha_0\hat{r}^0, -\hat{r}^0) \times e_{jk}^{S_2}(\mathbf{r}', \alpha_0\hat{z}, \hat{z})$$

where $\mathbf{u}^{S_2}$ is the exact solution *inside* a sphere of radius a_2 and $\mathbf{u}^{S_1}$ is the exact solution *outside* a sphere of radius a_1. Upon comparison of the right-hand side with the exact solution for

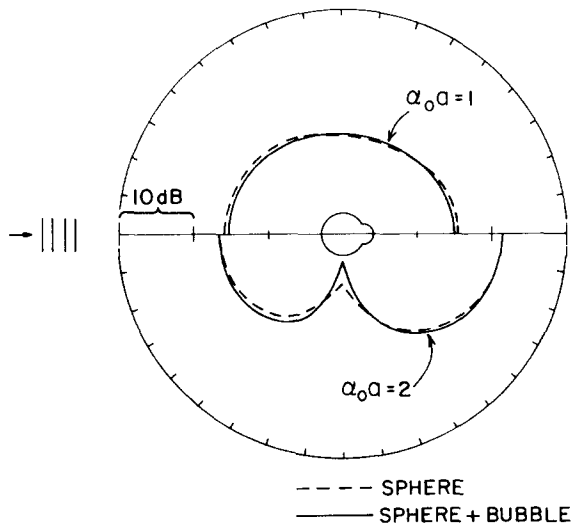

FIG. 13. Polar plot of power scattered from the defect of Fig. 9. The direction of incidence is $\theta_0 = 0$. The angular variation of the scattered power is shown for $\alpha_0 a = 1,2$. Same results for a spherical defect are also shown.

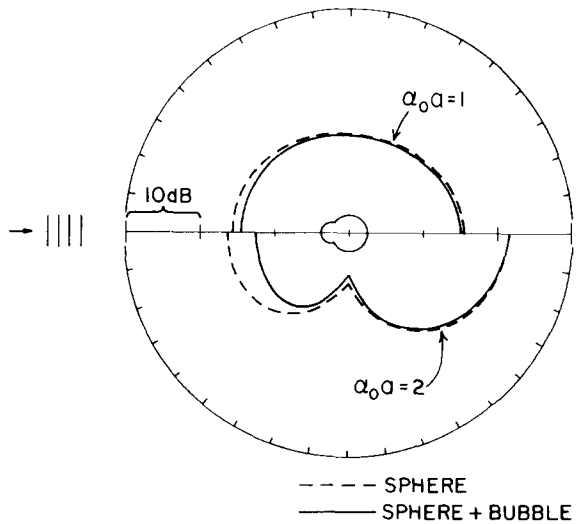

FIG. 14. Polar plot of power scattered from the defect of Fig. 9. The direction of incidence is $\theta_0 = 180°$. The angular variation of the scattered power is shown for $\alpha_0 a = 1,2$. Same results for a spherical defect are also shown.

scattering from a sphere of radius a_2 we found Eq. (4.9) to be satisfied with accuracy characteristic of our numerical integration procedure ($\sim 1\%$).

To study the accuracy of the DWBA, we calculated the scattering field from a sphere R using (4.1) and (4.2). This was done for Al spheres in Ti and for cavities in Ti. Two types of approximation were studied: the "full DWBA" is that of Eqs. (4.1) and (4.2) and an "intermediate DWBA" is the DWBA with an improper Green's function for the problem, namely, the infinite medium Green's function g^0 of Eq. (3.3). For elastic inclusions, parameters like $\delta\rho/\rho_0$ may be small and the intermediate DWBA is expected to work almost as well as the full DWBA. For cavities, the only small parameter in the calculation is $\delta V/V$, where δV is the volume of $\bar{R}$ and V the volume of S. For cavities, we tested the approximations with $a_2/a_1 = 1.2$, or $\delta V/V \cong 70\%$. For inclusions, we used $a_2/a_1 = 2$, which is an extremely nontrivial volume change of 700%.

The results of these checks are shown in Figs. 2–8. In these Figures "inner sphere" and "outer sphere" refer to the exact solution for spheres of radii a_1 and a_2, respectively. Scattered power or phase angle are plotted versus the dimensionless parameter $\alpha_0 a_2$. In general, the DWBA reproduces fairly well the exact results for the frequency and angular dependence of both power and phase. Note that "scattering angle" refers to the angle between the directions of incidence and observation. For the large perturbation $a_2/a_1 = 2$, the DWBA breaks down, for Al in Ti, at around $\alpha_0 a_2 > 3.5$. However, for $a_2/a_1 = 1.2$ the DWBA is good, even for a strong scatterer like a cavity, for a wide range of $\alpha_0 a_2$.

Next, we turn to study a nonspherical defect, shown in Fig. 9. The defect is a spherical cavity of diameter $2a = 800\mu$, to which a hemisphere cavity of diameter 400μ has been added. We will refer to the hemisphere as the "bubble"; it represents a deviation of size b from a simple shaped smooth cavity of characteristic size a. The questions we addressed are the following: (1) At what frequencies (e.g., values of $\alpha_0 b$) is the bubble observable? (2) At what angles of incidence and scattering is its effect most pronounced?

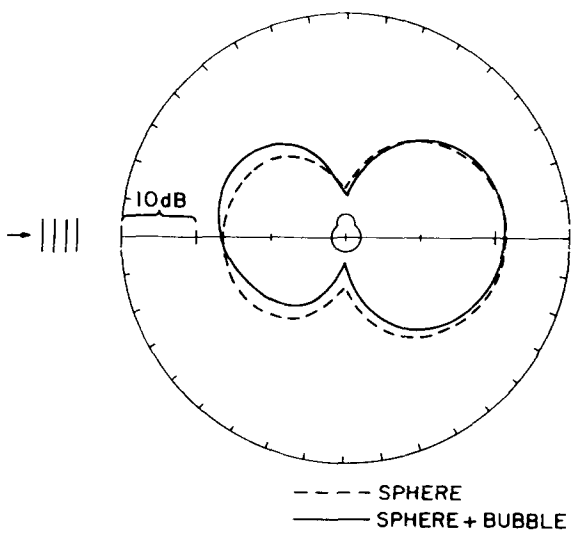

FIG. 15. Polar plot of power scattered from the defect of Fig. 9. The direction of incidence is $\theta_0 = 90°$. The angular variation of the scattered power is shown for $\alpha_0 a = 1,2$. Same results for a spherical defect are also shown. The scattered wave vector lies in the plane defined by the direction of incidence and the symmetry axis of the scatterer.

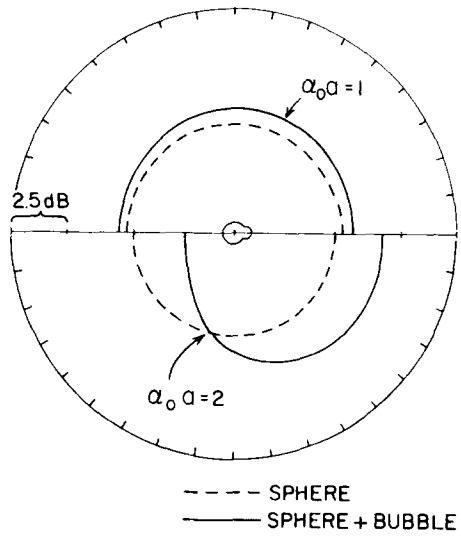

FIG. 16. Polar plot of power scattered from the defect of Fig. 9, as a function of the azimuthal scattering angle ϕ. The direction of incidence is $\theta_0 = 90°$, the scattered wave in the direction defined by $\theta = 135°$ and ϕ. Deviations from the symmetric pattern obtained from a sphere are sensitive to the deviation of the scatterer from spherical shape.

To answer these qeustions, we present, first, Figs. 10–12, which show the backscattered power versus $\alpha_0 a$ for three incident directions. These figures compare the scattering by the large sphere to that of the nonspherical defect. We find that experimentally observable differences (i.e., $\sim$3db) show up when $\alpha_0 a \approx 1.5$ (i.e., $\alpha_0 b \approx 0.75$). We also note tht the largest deviation is obtained for $\theta_0 = 180°$ (see Fig. 11), i.e., when the bubble is directly illuminated.

The frequency spectrum is modulated with about the same periodicity as that of a sphere, but a modulation with longer periodicity (in α_0) is superimposed. While for the sphere the first three peaks are of approximately equal amplitude, with the bubble present the amplitudes decrease in magnitude (for the first three peaks).

Turning now to angular distribution of power the sequence of Figs. 13–15 shows polar plots of power versus scattering angle for three directions of incidence, and $\alpha_0 a$ values of 1 and 2.

Again we note that the effect of the bubble is observable at $\alpha_0 a = 2$, and not at $\alpha_0 a = 1$. Also, the largest effect is obtained for $\theta_0 = 180$ (i.e., direct illumination), and even then the best results are obtained for backscattering.

It is of interest to observe the loss of symmetry of the scattered power, caused by the presence of the bubble. Figures 15 and 16 show this effect; in particular, the results of Fig. 16, with incidence at $\theta_0 = 90$ and scattering at $\theta = 135°$ have been verified experimentally.[18]

V. SUMMARY

The DWBA gives analytically simple forms for the scattering of elastic waves by defects of quite general shape. Numerical studies applying the DWBA to exactly solvable

shapes (spheres) indicate that the approximation yields reliable frequency dependence and phase information. The DWBA was applied to one irregularity shaped defect.

We plan to extend this work to the calculation of scattered shear waves. We would like to compare the results of this calculation with experiments; initial comparisons were most encouraging.[18] We would also like to use the DWBA to test some NDE inversion procedures[2,3,19] and the concept of defect representation by effective ellipsoids.

ACKNOWLEDGMENTS

This research was sponsored by the Center for Advanced NDE, operated by the Science Center, Rockwell International, for the Advanced Research Projects Agency and the Air Force Materials Laboratory under contract F33615-74-C-5180. We thank C. Kirschbaum and B. Yanoff for programing assistance.

[1]See, for example, *Proceedings of the ARPA /AFML Review of Progress in Quantitative NDE*, edited by D. O. Thompson, AFML-TR-78-205 (Air Force Materials Laboratory, 1979).
[2]J. H. Rose and J. A. Krumhansl, J. Appl. Phys. **50**, 2951 (1979).
[3]J. K. Cohen, N. Bleistein, and R. K. Elsley, *Proceedings of the ARPA /AFML Review of Progress in Quantitative NDE*, edited D. O. Thompson, AFML-TR-78-205 (1979), p. 454.
[4]W. Kohn and J. R. Rice, J. Appl. Phys. **50**, 3346 (1979).
[5]B. Budiansky and J. A. Rice, Trans. ASME J. Appl. Mech. **45**, 453 (1978).
[6]See Y. H. Pao and C. C. Mow, *Diffraction of Elastic Waves and Dynamic Stress Concentrations* (Crane, Russak, New York, 1971).
[7]J. E. Gubernatis, J. Appl. Phys. **50**, 4046 (1979).
[8]J. D. Achenbach, A. K. Gautesen, and H. McMaken, *Proceedings of the ARPA /AFML Review of Progress in Quantitative NDE*, edited by D. O. Thompson, AFML-TR-78-205 (1979), p. 321 and references therein.
[9]J. E. Gubernatis, E. Domany, J. A. Krumhansl, and M. Huberman, J. Appl. Phys. **48**, 2812 (1977).
[10]V. V. Varadan and V. K. Varadan, J. Acoust. Soc. Am. **63**, 1014 (1978).
[11]W. M. Visscher, J. Appl. Phys. **51**, 825 (1980); 835 (1980).
[12]C. F. Ying and R. Truell, J. Appl. Phys. **27**, 1086 (1956); G. Johnson and R. Truell, J. Appl. Phys. **36**, 3466 (1965); N. G. Einspruch, E. J. Witterholt, and R. Truell, J. Appl. Phys. **31**, 806 (1960). See also J. E. Gubernatis, E. Domany, J. A. Krumhansl, and M. Huberman, J. Appl. Phys. **48**, 2812 (1977).
[13]N. F. Mott and H. S. W. Massey, *The Theory of Atomic Collisions* (Oxford, New York, 1933), p. 100.
[14]J. E. Gubernatis, E. Domany, and J. A. Krumhansl, J. Appl. Phys. **48**, 2804 (1977).
[15]Note that for inclusions, $\bar{R}$ can also be defined to be a region *internal* to the sphere.
[16]K. E. Newman, C. K. Lam, and E. Domany (unpublished).
[17]J. E. Gubernatis (unpublished).
[18]B.R. Tittmann (unpublished).
[19]M. F. Whalen and A. N. Mucciardi, *Proceedings of the ARPA /AFML Review of Progress in Quantitative NDE*, edited by D. O. Thompson, AFML-TR-78-205 (1979), p. 341.